Extended Abstracts of the 2007 International Conference on Solid State Devices and Materials, Tsukuba, 2007, pp. 728-729

B-5-2

Physical Mechanism for Hole Mobility Enhancement in (110)-Surface Strained-Si/Strained-SiGe Structures with Anisotropic/Biaxial Strain

T. Mizuno[1,3], T. Irisawa[2], N. Hirashita[2], Y. Moriyama[2], T. Tezuka[2], N. Sugiyama[2], and S. Takagi[1,4]
[1]MIRAI-AIST, [2]MIRAI-ASET, 1 Komukai Toshiba-cho, Saiwai-ku, Kawasaki, Japan 212-8582
[3]Kanagawa University, 2946, Tsuchiya, Hiratsuka 259-1293, Japan (mizuno@info.kanagawa-u.ac.jp)
[4]The University of Tokyo, 7-3-1 Hongo, Bunkyo-ku, Tokyo 113-8656, Japan

I. Introduction

Recently, we have developed novel anisotropic strain engineering on the (110)-surface SSGOI (strained-Si on SGOI substrates) p-MOS devices, in order to enlarge the hole mobility enhancement factors even at high vertical electric field, using a combination of the global strain technique based on strained-SGOI substrates with the uniaxial relaxation across the narrow channels [1], [2]. However, the physical mechanism for the hole mobility enhancement in the anisotropic strained-SiGe/Si layers has not been understood, yet.

In this work, we clarify the physical mechanism for the hole mobility enhancement of MOSFETs along <110> current flow, which is the best channel direction, in both the anisotropic and the biaxial strained-SiGe/Si layers, by analyzing the lattice temperature T_L dependence. Moreover, we analyze the hole transport in (110)-surface biaxial and anisotropic strained-SiGe layers at both the strained-Si and the buried-oxide interfaces (back channel), which provides the significant contribution to the total current flow. By controlling the substrate bias V_B, we have studied the transport properties of the hole currents of three channels of SSGOIs, which are the front strained-Si (I_{Si}), strained-Si/SiGe interfaces (I_{SG}), and the SiGe back channels at the buried oxide interface (I_{BC}).

II. (110)-Anisotropic Strained-Si/Strained-SiGe Structures

Fig. 1 shows the schematic view of the present anisotropic strained Si/SiGe layers, using biaxial compressive strained-SGOI substrates. As shown in Fig.1 (b), a very narrow SiGe layer on a BOX layer is relaxed only across the best channel <110> direction, and still has compressive strain along the channel direction. As a result, a very narrow SiGe layer has uniaxial compressive strain, and a strained-Si layer formed on the narrow SiGe layer has anisotropic tensile strain.

(110)-SGOI substrates with the Ge content (x) of 34% were fabricated by the Ge condensation technique [1]. The SGOI (T_{SG}) and the strained-Si (T_{Si}) thicknesses were 50 nm and 13 nm, respectively. The narrow channel SSGOI and SOI regions with the minimum effective channel width W_{eff} of 0.2μm were formed by the mesa isolation process. Fully depleted SSGOI- and SOI-CMOS were fabricated by conventional CMOS processes. The channel dopant density was lower than 10^{16} cm^{-3}, and the gate oxide thickness was 8nm. As a result, the effective transverse field E_{eff} is mainly determined by the hole surface carrier density. The global SSGOI substrates have biaxial strain of 0.6%. As shown in Fig. 2, on the other hand, the strain value of the SiGe layers obtained by NBD analyses depends on W_{eff} along the <100> direction and rapidly increases with decreasing W_{eff}, when W_{eff} <0.8μm. As a result, the strained-Si and the SiGe layers with narrow W_{eff} have anisotropic tensile strain along <100> and uniaxial compressive strain along <110>, respectively. The maximum strain value along the <100> was 1.3% at W_{eff} of 0.2μm.

III. Hole Current Transport in Three Channels in SSGOIs

When the substrate bias V_B is set up to large minus values, the potential at the back channel becomes higher, resulting in hole currents (I_{BC}) at the back channel. Therefore, as shown in Fig.3, we can study the hole current transport of individual layers, that is, I_{Si} at the front strained-Si channel, I_{SG} at the buried strained-SiGe channel, and I_{BC}, by controlling V_B. In this study, we evaluate I_{Si}, I_{SG}, and I_{BC} at various T_L in comparison with I_{Si} and I_{BC} of conventional SOIs, in order to study the hole transport mechanism between the anisotropic and the biaxial SSGOIs.

IV. Field Effect Mobility Characteristics

In case of the anisotropic SSGOI channel, the split CV method cannot be used to determine the effective hole mobility, because of very narrow W_{eff}. In this work, thus, we evaluate the field effect hole mobility μ_F ($\equiv G_m L_{eff} T_{eff}/W_{eff} V_d \varepsilon_{ox}$, $T_{eff}=T_{ox}+T\varepsilon/\varepsilon_{ox}$), where T and ε are the thickness and the permittivity of layers, respectively, obtained by transconductance G_m. Fig.4 shows the G_m characteristics of anisotropic and biaxial SSGOIs and SOIs at low (25K) and room temperature (300K) with V_B=-10V. The G_m humps due to I_{Si}, I_{SG}, and I_{BC} in SSGOIs, and I_{Si} and I_{BC} in SOIs are clearly observed. However, the G_m humps due to I_{BC} disappears in SSGOIs at 25K. The G_m peak of anisotropic strained-Si layers is larger than that of biaxial strained-Si at both temperatures, although the G_m peak due to I_{SG} keeps constant in both strained-SiGe layers. On the other hand, the dips in G_m around V_g of -1V are observed in SSGOIs at low temperature, which is attributable to the gate oxide/Si interface states [3].

At first, the T_L dependence of μ_F of strained-SiGe layers and the μ_F enhancement factors against SOIs are shown in Fig.5, where the hole density N_s ($\equiv C_{ox}(V_g-V_{th})$) is 1×10^{12}cm^{-2}. It is found that that μ_F of strained-SiGe is largely enhanced against that of SOIs in the whole range of T_L and that the μ_F enhancement factors of around 2 are almost independent of T_L and anisotropic/biaxial strain configurations. These results suggest that the μ_F enhancement of both anisotropic and biaxial strained-SiGe channels is due to the effective mass reduction of holes.

On the other hand, the μ_F enhancement factors of strained-Si layers strongly depend on the strain configurations. As seen in Fig.6, μ_F of the anisotropic strained-Si is enhanced and the enhancement factors are between 1.2 and 1.5, which are smaller than those of strained-SiGe layers. In addition, the T_L dependence is very small, as similar to strained-SiGe layers. These results also suggest that the μ_F enhancement of the anisotropic strained-Si layers is caused by the reduced effective mass of holes. In case of biaxial strained-Si, however, μ_F is lower in the whole range of T_L than SOIs, which is attributable to the increased effective mass of holes in (110) surface biaxial strained-Si.

This reduction in the mobility is also seen in effective hole mobility μ_{eff}, evaluated from MOSFETs with large areas. Fig. 7 shows μ_{eff} of biaxial SSGOIs with L/W of 100 μm/100 μm as a function of N_s. The values of μ_{eff} are almost the same as μ_F of biaxial strained-Si/strained-SiGe layers mentioned above. The μ_{eff} ratio of biaxial strained-Si/strained-SiGe layers to SOIs is also independent of T_L. As a result, this μ_{eff} ratio is not attributable to any specific scattering mechanism of holes such as phonon scattering, but to the effective mass behaviors of biaxial SSGOIs.

Fig. 8 shows the back channel μ_F characteristics of anisotropic and biaxial strained-SiGe layers. The μ_F enhancement of both strain structures rapidly decreases with deceasing T_L, because μ_F of strained-SiGe layers rapidly decreases in the T_L range lower than 100K. On the other hand, μ_F of the back channel of SOIs is almost the same as that of the front channel. This μ_F reduction in SSGOIs is due to the Coulomb scattering caused by higher interface state density at the buried oxide interfaces. The interface states can be associated with the GeO_x formation at the SiGe/buried-oxide interfaces during the oxidation process of SiGe layers in the Ge condensation processes. Consequently, further improvement of the back interface properties is needed for utilizing I_{BC} of SSGOI MOSFETs as a device operation.

V. Optimum Anisotropic SSGOIs

Fig.9 shows the μ_F enhancement behaviors in strained-Si/strained-SiGe layers as a function of W_{eff} in various T_L. The μ_F enhancement factors of strained-SiGe layers are independent of W_{eff} and T_L However, the μ_F enhancement factors of strained-Si rapidly increases with decreasing W_{eff}. In addition, the μ_F ratio of strained-SiGe to strained-Si rapidly decreases in the anisotropic strain region. However, the strained-SiGe is the best channel structures for higher hole mobility.

To improve the performance of SSGOIs by utilizing the high hole mobility of strained-SiGe layers, the T_{Si} should be thinner. Namely, it is necessary that $I_{SG} \geq I_{Si}$. So, $v_{SG}/v_{Si} \geq (1+\varepsilon_{ox}T_{Si}/\varepsilon_{Si}T_{ox})$, where v_{SG} and v_{Si} are hole velocity of strained-SiGe and Si in scaled MOSFETs, respectively. On the other hand, T_{Si} has a lower limitation to prevent the GeO_x formation at the gate insulator [4]. Fig.10 shows successfully optimum design of T_{Si} for 18nm SSGOIs.

VI. Conclusion

We have studied the hole current transport in the three channels (I_{Si}, I_{SG}, and I_{BC}) of strained-Si/strained-SiGe layers in both the anisotropic and the biaxial SSGOIs, by controlling V_B in various T_L. It has been found through the field effect mobility at various temperatures that the hole mobility enhancement is explained by the effective mass reduction of holes. It is necessary to optimize T_{Si} to utilize strained-SiGe layers for high performance SSGOIs.

Acknowledgement: We would like to thank Drs. M.Hirose and T.Kanayama for their continuous supports. This was supported by NEDO.

References: [1]T.Mizuno et al., *IEDM Tech. Dig.*, p.453 (2006). [2] T. Irisawa et al., *VLSI Symp. Tech. Dig.*, p.178, 2005. [3] T.Mizuno et al., ED-51, 1114, 2004. [4] M.J. Palmer et al., APL, 78, 1424, 2001. [5] R.Ohba et al., ED-48, 338, 2001.

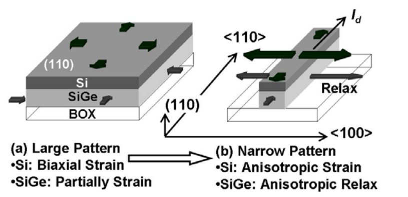

Fig.1 (a) Biaxial and (b) anisotropic strained-Si/strained-SiGe structures.

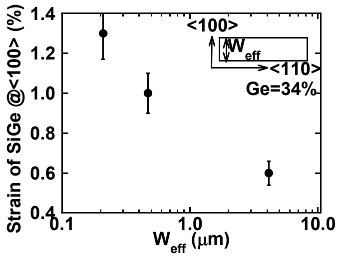

Fig.2 Strain value $\Delta a/a_{Si}$ of SiGe layers on BOX vs. W_{eff} along the <100> direction, analyzed by NBD analysis. The inset shows the schematic plane view of the measurement SGOI rectangular pattern with W_{eff}

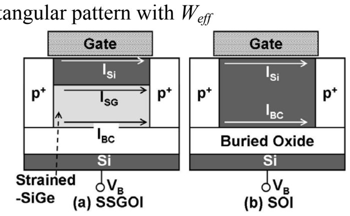

Fig.3 By controlling V_B, we have studied hole current transport of (a) three channels of SSGOIs and (b) two channels of SOIs, that is, front strained-Si in SSGOIs and Si in SOIs (I_{Si}), buried strained-SiGe channel in SSGOIs (I_{SG}), and the back channel (I_{BC}) in both devices.

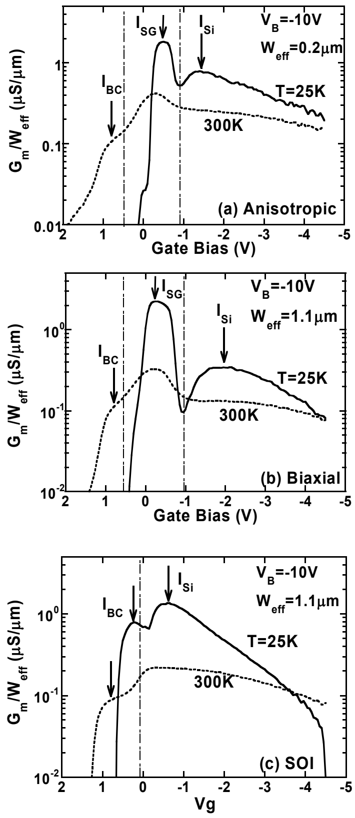

Fig.4 G_m characteristics normalized by W_{eff} of (a) anisotropic SSGOIs with W_{eff}=0.2μm, (b) biaxial SSGOIs with W_{eff}=1.1μm, and (c) SOIs with W_{eff}=1.1μm, where L_{eff}=4μm, V_d=–10mV, and V_B=–10V. The solid and the dashed lines show the experimental data at lattice temperature of 25K and 300K, respectively. Arrows indicate the G_m due to each channel shown in Fig.3.

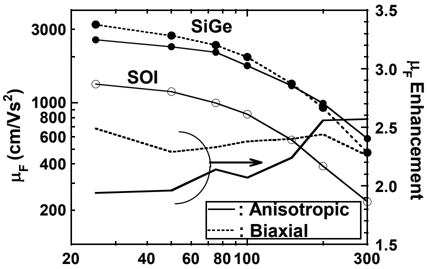

Fig.5 Field effect hole mobility μ_F (left axis) of strained-SiGe layers (closed circles) and SOIs (open circles), and μ_F enhancement factors (dashed line) of strained-SiGe (right axis) against SOIs vs. temperature, where μ_F was obtained by G_m and hole density N_s is 1×10^{12}cm^{-2}. The solid and the dashed lines show the data of anisotropic (W_{eff}=0.2μm) and biaxial (W_{eff}=1.1μm) strained-SiGe layers, respectively.

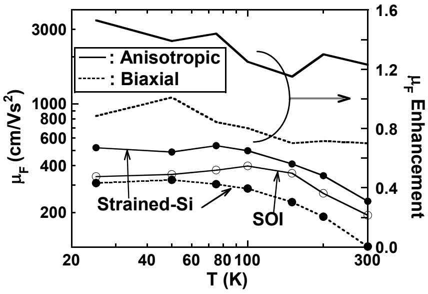

Fig.6 μ_F (left axis) of strained-Si layers (closed circles) and SOIs (open circles), and μ_F enhancement factors (dashed line) of strained-Si (right axis) vs. temperature, where N_s=5.5×10^{12}cm^{-2}. The solid and the dashed lines show the data of anisotropic (W_{eff}=0.2μm) and biaxial (W_{eff}=1.1μm) strained-Si layers, respectively.

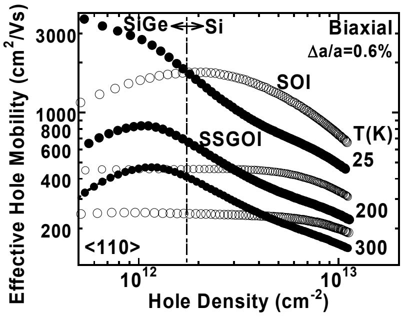

Fig.7 Effective hole mobility vs. N_s of biaxial SSGOIs (closed circles) and SOIs (open circles) in various temperature, where $L_{eff}=W_{eff}$=100μm and V_d=–10mV, hole mobility was obtained by conventional usual split CV method. The hole mobility at N_s of less than 1.8×10^{12}cm^{-2} originates from the strained-SiGe layers.

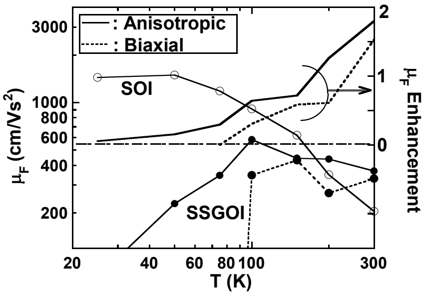

Fig.8 Back channel μ_F (left axis) of strained-SiGe layers (closed circles) and SOIs (open circles), and μ_F enhancement factors (dashed line) of strained-SiGe (right axis) vs. temperature, where N_s=1×10^{12}cm^{-2}. The solid and the dashed lines show the data of anisotropic (W_{eff}=0.2μm) and biaxial (W_{eff}=1.1μm) strained-SiGe layers, respectively.

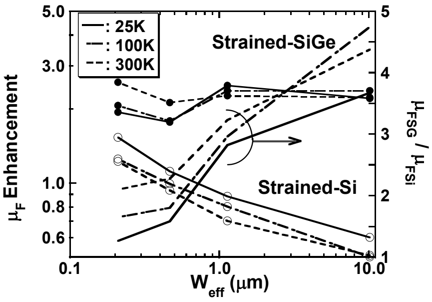

Fig.9 μ_F enhancement factors (left axis) of strained-SiGe and Si layers against SOIs vs. W_{eff} in various temperatures. The right axis shows the μ_F ratio of strained-SiGe to strained-Si. In the biaxial strain region, the μ_F ratio is larger than 4. However, the μ_F ratio rapidly decreases to 1.2 in the anisotropic strain region.

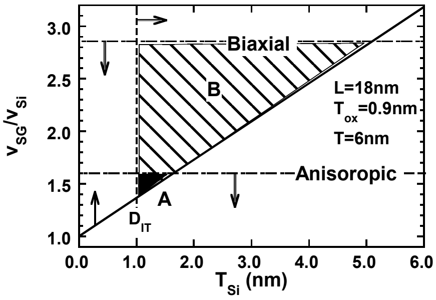

Fig.10 Device design of T_{Si} for 18nm SSGOIs, utilizing a high hole mobility of strained-SiGe layers, where T_{ox}=0.9nm. The vertical axis shows the hole velocity ratio of strained-SiGe to strained-Si layers, v_{SG}/v_{Si}. The total thickness T of strained-Si/SiGe layers should be thinner than L/3, to suppress the short channel effects. In order to prevent the D_{IT} generation by the diffused Ge atoms from the SiGe layers, it is assumed that $T_{Si}\geq$1nm (dashed line) [4]. The solid line shows the condition that $v_{SG}/v_{Si}\geq(1+T_{Si}/3T_{ox})$. The dotted lines indicate the upper limit of v_{SG}/v_{Si}, which is calculated by using the power law of carrier mobility [5] and the μ_F ratio shown in Fig.9. As a result, region A (shadow area) and B (hatching area) show the optimum region for SSGOIs with anisotropic and biaxial SSGOIs, respectively. The high hole mobility of strained-SiGe layers is very useful for improving biaxial SSGOIs, because the hole mobility of biaxial strained-Si is lower. On the other hand, the optimum T_{Si} range for anisotropic SSGOIs is very narrow, because of relatively small v_{SG}/v_{Si}.